

AD

TECHNICAL REPORT ARCCB-TR-95008

RESIDUAL STRESS EFFECTS AT A NOTCH ROOT IN A723 STEEL TO EXTEND FATIGUE LIFE

J.H. UNDERWOOD



FEBRUARY 1995



**US ARMY ARMAMENT RESEARCH,
DEVELOPMENT AND ENGINEERING CENTER**
CLOSE COMBAT ARMAMENTS CENTER
BENÉT LABORATORIES
WATERVLIET, N.Y. 12189-4050



APPROVED FOR PUBLIC RELEASE; DISTRIBUTION UNLIMITED

DTIC QUALITY INSPECTED 6

19950519 019

DISCLAIMER

The findings in this report are not to be construed as an official Department of the Army position unless so designated by other authorized documents.

The use of trade name(s) and/or manufacturer(s) does not constitute an official indorsement or approval.

DESTRUCTION NOTICE

For classified documents, follow the procedures in DoD 5200.22-M, Industrial Security Manual, Section II-19 or DoD 5200.1-R, Information Security Program Regulation, Chapter IX.

For unclassified, limited documents, destroy by any method that will prevent disclosure of contents or reconstruction of the document.

For unclassified, unlimited documents, destroy when the report is no longer needed. Do not return it to the originator.

REPORT DOCUMENTATION PAGE

Form Approved
OMB No. 0704-0188

Public reporting burden for this collection of information is estimated to average 1 hour per response, including the time for reviewing instructions, searching existing data sources, gathering and maintaining the data needed, and completing and reviewing the collection of information. Send comments regarding this burden estimate or any other aspect of this collection of information, including suggestions for reducing this burden, to Washington Headquarters Services, Directorate for Information Operations and Reports, 1215 Jefferson Davis Highway, Suite 1204, Arlington, VA 22202-4302, and to the Office of Management and Budget, Paperwork Reduction Project (0704-0188), Washington, DC 20503.

1. AGENCY USE ONLY (Leave blank)		2. REPORT DATE February 1995		3. REPORT TYPE AND DATES COVERED Final	
4. TITLE AND SUBTITLE RESIDUAL STRESS EFFECTS AT A NOTCH ROOT IN A723 STEEL TO EXTEND FATIGUE LIFE				5. FUNDING NUMBERS AMCMS: 6111.02.H611.1	
6. AUTHOR(S) J.H. Underwood					
7. PERFORMING ORGANIZATION NAME(S) AND ADDRESS(ES) U.S. Army ARDEC Benét Laboratories, AMSTA-AR-CCB-O Watervliet, NY 12189-4050				8. PERFORMING ORGANIZATION REPORT NUMBER ARCCB-TR-95008	
9. SPONSORING/MONITORING AGENCY NAME(S) AND ADDRESS(ES) U.S. Army ARDEC Close Combat Armaments Center Picatinny Arsenal, NJ 07806-5000				10. SPONSORING/MONITORING AGENCY REPORT NUMBER	
11. SUPPLEMENTARY NOTES Published in <i>Experimental Mechanics</i> , March 1995.					
12a. DISTRIBUTION/AVAILABILITY STATEMENT Approved for public release; distribution unlimited				12b. DISTRIBUTION CODE	
13. ABSTRACT (Maximum 200 words) Fatigue life tests were performed with notched bend specimens of ASTM A723 steel with three types of residual stress treatments and resulting residual stress: shot peening, hole swaging, and tensile overload. The three treatments produced widely different depths and surface values of residual stress near the notch root and different fatigue lives depending mainly on the notch root surface value of compressive residual stress. The highest life was measured from overload specimens, which had both the deepest and the highest surface value residual stress distribution. Fracture mechanics-based calculations of fatigue life agreed well with measurements. The calculations accounted for the following factors that affect fatigue life: the crack growth properties of the material; the shallow surface-crack configuration; the applied loading; and the depth and surface magnitude of the residual stress distribution. A consistent description of fatigue life was obtained from a ΔK versus calculated life plot, where the ΔK is for a shallow crack near the notch root and in the region of compressive residual stress. A power-law relationship between ΔK and fatigue life agreed well with the results from both the untreated notches and those with the three types of residual stress, indicating that fatigue life predictions could be made with some confidence for tests under generally similar conditions.					
14. SUBJECT TERMS Residual Stress, Fatigue Life, Crack Growth, Notch Root, Shot Peening, Tensile Overload, Hole Swaging, Notched Bend Specimens				15. NUMBER OF PAGES 16	
				16. PRICE CODE	
17. SECURITY CLASSIFICATION OF REPORT UNCLASSIFIED	18. SECURITY CLASSIFICATION OF THIS PAGE UNCLASSIFIED	19. SECURITY CLASSIFICATION OF ABSTRACT UNCLASSIFIED	20. LIMITATION OF ABSTRACT UL		

TABLE OF CONTENTS

ACKNOWLEDGEMENTS	ii
INTRODUCTION AND OBJECTIVE	1
SPECIMEN, MATERIAL, AND TEST	1
TYPES OF RESIDUAL STRESS	1
FATIGUE LIFE TESTS AND CALCULATIONS	2
Life Tests	2
Life Calculations	3
SUMMARY	5
REFERENCES	6

Tables

1. Test Conditions and Residual Stress Distribution For Notched Fatigue Specimens	7
2. Comparison of Measured and Calculated Crack Growth Lives and Total Lives For Notched Fatigue Specimens	8

List of Illustrations

1. Specimen configuration	9
2. Measured residual stress for swaged and machined specimen	10
3. Model of elastic-plastic stresses due to overload of notch	11
4. Typical residual stress distributions ahead of notch	12
5. Measured fatigue crack growth for various notch root treatments	13
6. Comparison of measured and calculated fatigue lives	14

ACKNOWLEDGEMENTS

The author is pleased to acknowledge the work of the late John Zalinka, who performed all the tests described here, and the help and advice in all phases of the work of the late Joseph Throop.

Accession For	
NTIS CRA&I	<input checked="checked" type="checkbox"/>
DTIC TAB	<input type="checkbox"/>
Unannounced	<input type="checkbox"/>
Justification _____	
By _____	
Distribution /	
Availability Codes	
Dist	Avail and/or Special
A-1	

INTRODUCTION AND OBJECTIVE

Several years ago results of fatigue tests in pressurized cylinders and in notched bending samples of high strength steel were described (ref 1) with emphasis on residual stress effects on fatigue crack growth and fatigue life. Today there is a continued interest in the effects of residual stress on fatigue life of many types of structural components, including large caliber gun components. Despite concerted attempts, the designer can never eliminate all stress concentrations and notches in a structural component that has any sort of practical use, and residual stresses can greatly extend the fatigue life at a notch. The objectives here are to describe three methods of introducing plastic deformation at a notch and the residual stresses that are produced in an A723 steel and to give the results of notch fatigue tests with the three types of notch treatment. Some of the results from Reference 1 are used as a basis for the work here, with additional results and descriptions given of the notch-root plastic deformation, the residual stresses, and the calculation of fatigue lives for comparison with measured lives.

SPECIMEN, MATERIAL, AND TEST

The failure of many cannon components is by fatigue crack growth that initiates at a notch of some type. A pragmatic approach sometimes used in the design of cannon components is that notches are inevitable, so make them as harmless as possible. This was the approach that led to the tests described in this work, as shown in Figure 1. A large radius notch, 12.5 mm, was used. It was intended to be the typical size notch of cannon components with improved fatigue life design corresponding to a large radius. The fatigue life would be further enhanced using residual stress, as discussed later. The notch was made by carefully machining a 25-mm diameter hole near the midwall position of half sections of a single thick-walled cylinder and then machining a cutout to form a semicircular notch. The cylinder material was the pressure vessel steel commonly used for gun tubes, A723 steel, quenched and tempered to 1030 MPa yield strength and 1140 MPa tensile strength. The test plan was to apply tension-to-tension load cycles to specimens with various notch surface treatments and associated residual stress distributions. The initiation and growth of a surface crack of length $2c$ would be monitored, and the fatigue lives would be related to the levels of residual stress.

TYPES OF RESIDUAL STRESS

The three types of residual stress treatments were shot peening, hole swaging, and notch overload, as shown in Table 1. The shot peening was performed in the usual manner, with the entire notch surface peened to an Almen intensity of 0.008A for one sample and 0.015A for another. The expected depth of the residual stress distribution, a_o , (to the point of zero stress) and the stress value at the surface, S_o , were obtained from the literature (ref 2) for similar conditions, 0.0085A and 0.014A intensities, in an AISI 4340 steel.

The hole swaging was performed by forcing an oversized, hard steel ball through the 25-mm hole such that there was a permanent bore enlargement of the hole: 0.4 percent for one sample and 1.4 percent for another. The residual stress distributions that resulted from the swage operations were characterized by X-ray diffraction measurements (ref 3) around the hole

after swaging and resistance strain gage measurements on the hole's inside diameter (ID) surface before and after the cutout machining. Figure 2 shows the X-ray measurements for the 0.4 percent bore enlargement specimen and the modification to the X-ray results due to the strain increment caused by machining the cutout. The resulting values of a_o and S_o are listed in Table 1 for the two swaged specimens.

The overload was performed by simply applying a single tensile preload of about twice the maximum load value planned for the subsequent fatigue testing. Prior work (ref 4) showed that a tensile overload of twice the maximum fatigue load produced enough compressive residual stresses at the notch root to significantly extend fatigue life. A simple elastic-plastic stress model was developed to calculate the depth, a_o , and surface magnitude, S_o , of residual stress due to an overload, as seen in Figure 3. Referring to Figure 1, the following expression can be written for the sum of the normal and bending elastic stresses ahead of the notch, S_x , as a function of position x :

$$S_x = [P/Bb][1 + 12xL/b^2] \quad (1)$$

The depth, a_o , of the residual stress distribution can be determined from Eq. (1) by calculating the x value at which $S_x = S_y$, the yield strength, 1040 MPa. For $S_x = S_y$ and for the B , b , and L values in Figure 1, $a_o = 5.7$ and 7.6 mm for overloads of 45.8 and 56.0 KN, respectively. These overloads are 1.8 and 2.2 times the P_{max} to be used subsequently in the fatigue tests. The surface magnitude of residual stress, S_o , is calculated by assuming that the unloading is linear and complete, so that

$$S_o = -(S_n - S_y) \quad (2)$$

where S_n represents the elastic notch root stress that would be obtained if no yielding occurred. The values of S_o from Eq. (2) are -560 and -910 MPa tangential direction residual stress at the notch root, respectively, for the above-mentioned overloads.

Typical residual stress distributions--for shot peen, hole swage, and tensile overload conditions--are plotted in Figure 4. Some approximations were made in determining the residual stresses, as discussed above. However, the residual stresses are believed to be close enough to the actual values to give useful information on the effects of residual stress depth and surface magnitude on fatigue life. Note in Figure 4 and Table 1 that S_o varies by about a factor of three and a_o varies by more than a factor of ten over the range of test conditions. These significant differences in residual stress distribution should be reflected in the results of the fatigue life tests.

FATIGUE LIFE TESTS AND CALCULATIONS

Life Tests

Eight tests were performed, as seen in Table 2. The same configuration, Figure 1, and the same maximum and minimum loads, 25.4 and 2.54 KN, were used for all tests. A florescent magnetic particle inspection method, ultraviolet light, and low power telescope were used to monitor the notch root during the fatigue tests. Typically, a surface crack of about 1 mm was

detected near the center of the notch root and monitored until it had grown across the full 25.4-mm width of the root, at which point final failure of the specimen was imminent within a few hundred cycles. Plots of the ratio $2c/B$ versus the cycle count are shown in Figure 5. The plot for no surface treatment is a composite of two tests for this condition; all other plots are from a single specimen. Two features of these plots that may be of particular interest are the total number of cycles to failure and the number of cycles required to grow the crack from first detection, $2c/B = 0.05$, to a length one-quarter of the specimen thickness, $2c/B = 0.25$. This latter crack growth life may be particularly sensitive to the residual stress differences near the notch root. The measured total fatigue lives and the $2c/B = 0.05 - 0.25$ growth lives are listed in Table 2. These life comparisons are believed to be unaffected by material and machining differences, because all specimens were machined with care from the same cylinder.

Note that for the shot peened specimens, for example, the growth lives are relatively low and the total lives are relatively high. This can probably be explained by the relatively shallow depths and relatively high surface levels of the peen residual stresses indicated in Table 1. For the swage specimens, the growth lives are greater than those for the peen specimens, but the total life for the highly swaged specimen is only half that of the highly peened specimen. This indicates that the surface level of residual stress (relatively low for the swage specimens) is a more important determinant of fatigue life than the depth of residual stress. For the overload specimens, which had both a relatively deep and a relatively high surface level residual stress, both the growth lives and the total lives were the highest of all the tests.

Life Calculations

Calculations of fatigue life for these specimens may be of use. If simple yet general calculations of fatigue life could be made and shown to agree well with the measured lives, then the calculations could be used for other configurations, materials, or test conditions, and would be useful for design or guidance in testing. Calculations were made using a fracture mechanics approach, starting with an experimentally-determined relationship for the fatigue crack growth rate for the A723 steel with stress ratio, R , of 0.1⁵

$$da/dn = 6.52 \times 10^{-12} (\Delta K)^3 \quad (3)$$

In Eq. (3) ΔK is the applied range of stress intensity factor in the fatigue crack growth rate tests, and the numerical constants apply for da/dn in m/cycle and K in $\text{MPa m}^{1/2}$. The effective range of K in the fatigue life tests is defined as

$$\Delta K_{EFF} = K_{MAX} + K_{RES} \quad (4)$$

where the K expressions for the applied K range, ΔK , and the residual stress, K_{RES} , are

$$\Delta K = 1.12 h \Delta S_n (\pi a)^{1/2} \quad (5)$$

$$\begin{aligned} K_{RES} &= 0.44 h S_o (\pi a)^{1/2} & \text{for } a < a_o \\ &= 0 & \text{for } a > a_o \end{aligned} \quad (6)$$

Equation (5) is the familiar expression for a shallow crack with an applied tensile stress, S_n , and it can be used to describe a shallow surface crack by adding the factor h to account for the semi-elliptical shape of the crack. For the tests here, the ratio of depth to total surface length of the crack, $a/2c$, was typically 0.3 for the early growth of the crack that has primary control of fatigue life. Newman and Raju (ref 6) give an $h = 0.78$ for $a/2c = 0.3$. Equation (6) is from the Benthem and Koiter solution (ref 7) for an edge crack in a linear-varying stress distribution; recall from Figure 4 that the residual stress distributions are well approximated by a linear distribution, at least for $a < a_o$. Equation (6) is believed to be a lower bound estimate of K_{RES} over the range $a_i < a < a_o$. For $a > a_o$, the residual stress is tensile and is assumed to have no significant effect on ΔK .

Equations (4) through (6) account for a decrease in ΔK_{EFF} due to a compressive residual stress, but they do not account for any changes in ΔK_{EFF} due to a tensile residual stress. Methods and models are available that could account for the effect of tensile residual stress and other effects, but their use would not result in a simple rational expression for fatigue life, which was the intended approach here.

Equation (3) can be easily integrated in closed form and combined with Eqs. (4) through (6) to yield an expression for fatigue life, N , that accounts for the initial and final crack depth, a_i and a_f ; the crack growth rate properties of the material; the shallow surface crack configuration; the applied loading, bending in this case; and the depth and surface magnitude of the residual stress distribution. The expression is

$$\begin{aligned} N &= 2 \left[1/(a_i)^{1/2} - 1/(a_f)^{1/2} \right] / 6.52 \times 10^{-12} (\pi)^{1/2} f h S_n^3 \\ f &= 1.12 & \text{for } a > a_o \\ f &= 1.12 + 0.44 (S_o/S_n) & \text{for } a < a_o \end{aligned} \quad (7)$$

Equation (7) was used to calculate fatigue lives for comparison with the experimental results with the following inputs: $a_i = 0.02$ mm; $a_f = 7.5$ mm ($a_f = 0.3 B = 0.3 \{25 \text{ mm}\}$, to account for the $a/2c = 0.3$ crack shape); $h = 0.78$ (as discussed previously); S_o and a_o from Table 1; and $S_n = 880$ MPa (from Eq. (1) for $P_{max} = 25.4$ KN and $x = b/2$). The only arbitrarily selected input was $a_i = 0.02$ mm, and this is in reasonable agreement with the value used (0.01 mm) in recent similar life calculations (ref 8). There is some reason to expect that the notch here was not as finely machined as the specimens in the recent work, so the somewhat larger a_i may be justified.

The comparison of calculated and measured fatigue lives is shown in Table 2. The growth life for $2c/B = 0.05 - 0.25$ was calculated from Eq. (7) using $a = 0.38 - 1.90$ mm (for example, $a_i = \{0.05\}\{0.3\}\{25 \text{ mm}\} = 0.38$ mm); the measured growth life for the same range of a was taken from the plots of Figure 5. It can be seen that the calculated growth life

overestimates the measured growth life by about 30 to 100 percent. The comparison of total fatigue life shows better agreement, with calculated life varying from about 25 percent low to 40 percent high. The average difference is a calculated life only about 3 percent below measured life.

A final comparison of measured and calculated fatigue lives is shown in Figure 6. The measured and calculated total lives from Table 2 are plotted (as a log-log plot) versus the ΔK_{EFF} value from Eq. (4) for $a = 0.3$ mm. The $a = 0.3$ mm value was chosen as a crack depth within the compressive residual stress region for all the specimens, as well as a relatively shallow crack depth. The ΔK at such a shallow depth may relate well to fatigue life, because a significant portion of life occurs at shallow depth. The plot of Figure 6 shows visually the relatively good agreement between calculated and measured life already discussed in relation to Table 2. Figure 6 also shows that calculated life is well represented by a linear regression line, which (on this log-log plot) indicates a power-law relationship between $\Delta K_{a=0.3\text{ mm}}$ and fatigue life. This means that the expressions for K and fatigue life developed here give a consistent description of the fatigue life behavior and could thus be used with some confidence for fatigue life predictions in similar tests and components. Such predictions would include factors that affect fatigue life included in Eq. (7) and discussed here, namely, the crack growth properties of the material; the shallow surface crack configuration; the applied loading; and the depth and surface value of the residual stress distribution.

SUMMARY

1. Fatigue life tests were performed with notched bend specimens of A723 steel with three types of notch treatments and resulting residual stress: shot peening, hole swaging, and tensile overload. The three notch treatments produced widely different depths and surface values of residual stress near the notch root and different fatigue lives depending mainly on the magnitude of the compressive residual stress at the notch root surface. The highest life was measured from overload specimens that had both the deepest residual stress distribution and the highest surface magnitude of residual stress.

2. Fracture mechanics-based calculations of fatigue life agreed well with measurements for all notch treatments. The calculations accounted for the following factors that affect fatigue life: the crack growth properties of the material; the shallow surface crack configuration; the applied loading; and the depth and surface magnitude of the residual stress distribution.

3. A consistent description of fatigue life was obtained from a ΔK versus calculated life plot, where the ΔK is for a shallow crack near the notch root and in the region of compressive residual stress. A power-law relationship between ΔK and life agreed well with the results from both the untreated notches and those with the three types of residual stress, indicating that life predictions could be made with some confidence for tests with similar conditions to those considered here.

REFERENCES

1. J.H. Underwood and J.F. Throop, "Residual Stress Effects on Fatigue Cracking of Pressurized Cylinders and Notched Bending Specimens," *Proceedings of 1980 SESA Spring Meeting*, Boston, May 1980.
2. Helmut Wohlfahrt, "Shot Peening and Residual Stress," *Residual Stress and Stress Relaxation*, (Eric Kula and Volker Weiss, Eds.), Plenum, 1982, pp. 71-92.
3. Keith Loomis, unpublished results, U.S. Army Armament Research, Development, and Engineering Center, Watervliet, NY.
4. J.H. Underwood and J.A. Kapp, "Benefits of Overload for Fatigue Cracking at a Notch," *Fracture Mechanics: Thirteenth Conference, ASTM STP 743*, (Richard Roberts, Ed.), American Society for Testing and Materials, 1982, pp. 48-62.
5. J.H. Underwood and J.F. Throop, "Surface Crack K Estimates and Fatigue Life Calculations in Cannon Tubes," *Part-Through Crack Fatigue Life Prediction, ASTM STP 687*, (J.B. Chang, Ed.), American Society for Testing and Materials, 1979, pp. 195-210.
6. J.C. Newman, Jr. and I.S. Raju, "An Empirical Stress-Intensity Factor Equation for the Surface Crack," *Engineering Fracture Mechanics*, Vol. 15, 1981, pp. 185-192.
7. J.P. Benthem and W.T. Koiter, "Asymptotic Approximations to Crack Problems," *Methods of Analysis of Crack Problems*, (G.C. Sih, Ed.), Noordhoff International, Leyden, The Netherlands, 1972.
8. A.P. Parker and J.H. Underwood, "Stress Concentration, Stress Intensity, and Fatigue Crack Growth Along Evacuators of Pressurized, Autofrettaged Tubes," U.S. Army ARDEC Technical Report ARCCB-TR-94046, Watervliet, NY, December 1994.

**Table 1. Test Conditions and Residual Stress Distribution
For Notched Fatigue Specimens**

Treatment	Level of Treatment	Residual Stresses	
		Depth a_o , mm	S at Surface S_o , MPa
None	-	-	-
Peen	Almen intensity 0.008A	0.33	-730
	Almen intensity 0.015A	0.46	-900
Swage	0.4% bore enlargement	3.8	-250
	1.4% bore enlargement	6.5	-430
Overload	1.8 times P_{max} of fatigue	5.7	-560
	2.2 times P_{max} of fatigue	7.6	-910

**Table 2. Comparison of Measured and Calculated Crack Growth Lives
and Total Lives For Notched Fatigue Specimens**

Treatment	Life for $2c/B = 0.05 - 0.25$		Total Fatigue Life	
	N_{MEAS} Cycles	N_{CALO}/N_{MEAS}	N_{MEAS} Cycles	N_{CALO}/N_{MEAS}
None: #1	-	-	28,000	-
#2	-	-	31,500	-
mean	3,400	1.91	29,800	0.86
Peen: low	3,900	1.62	51,000	1.41
high	5,500	1.76	105,500	0.99
Swage: low	6,000	2.03	47,800	0.76
high	8,900	1.49	52,500	0.93
Overload: low	10,900	1.51	62,500	0.97
high	22,900	1.32	143,000	0.86

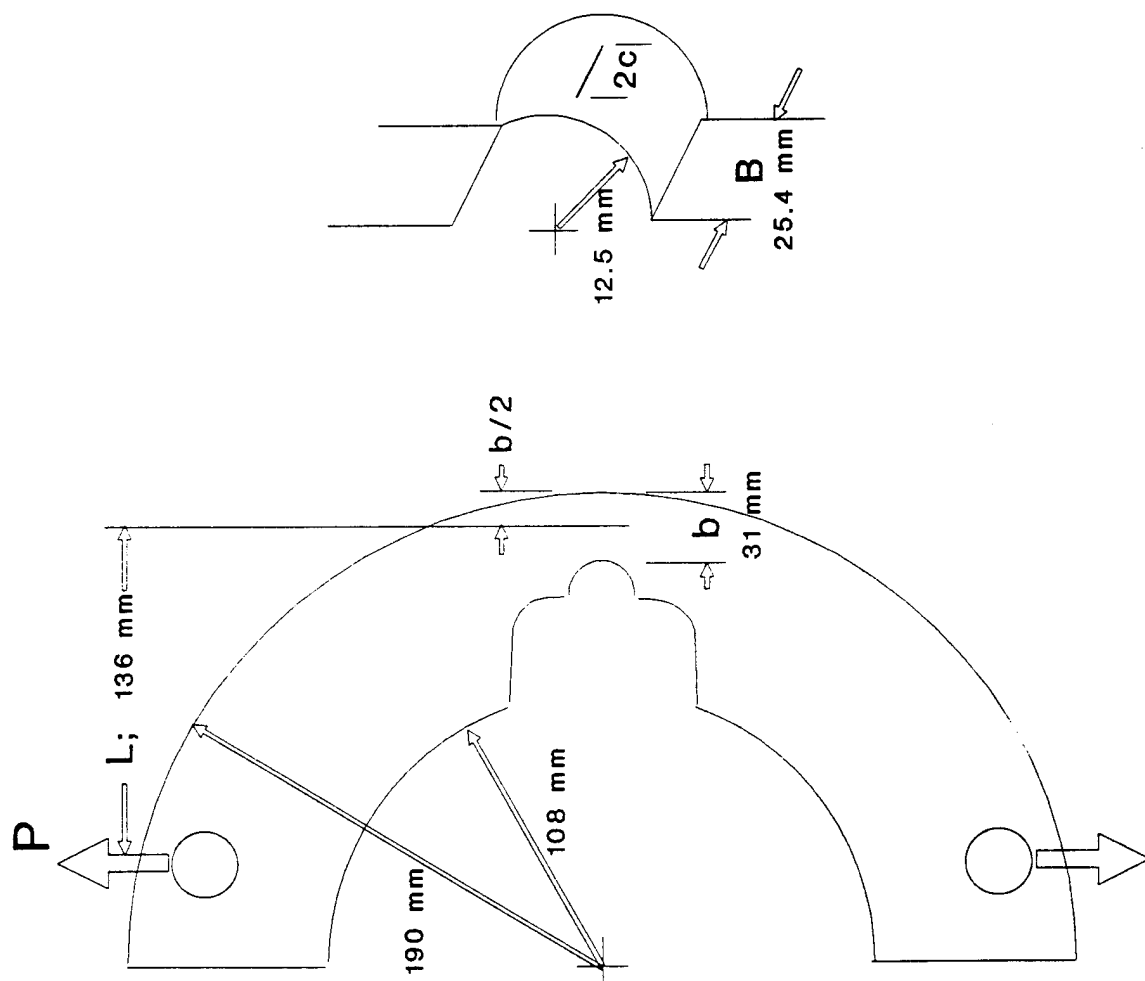


Figure 1. Specimen configuration.

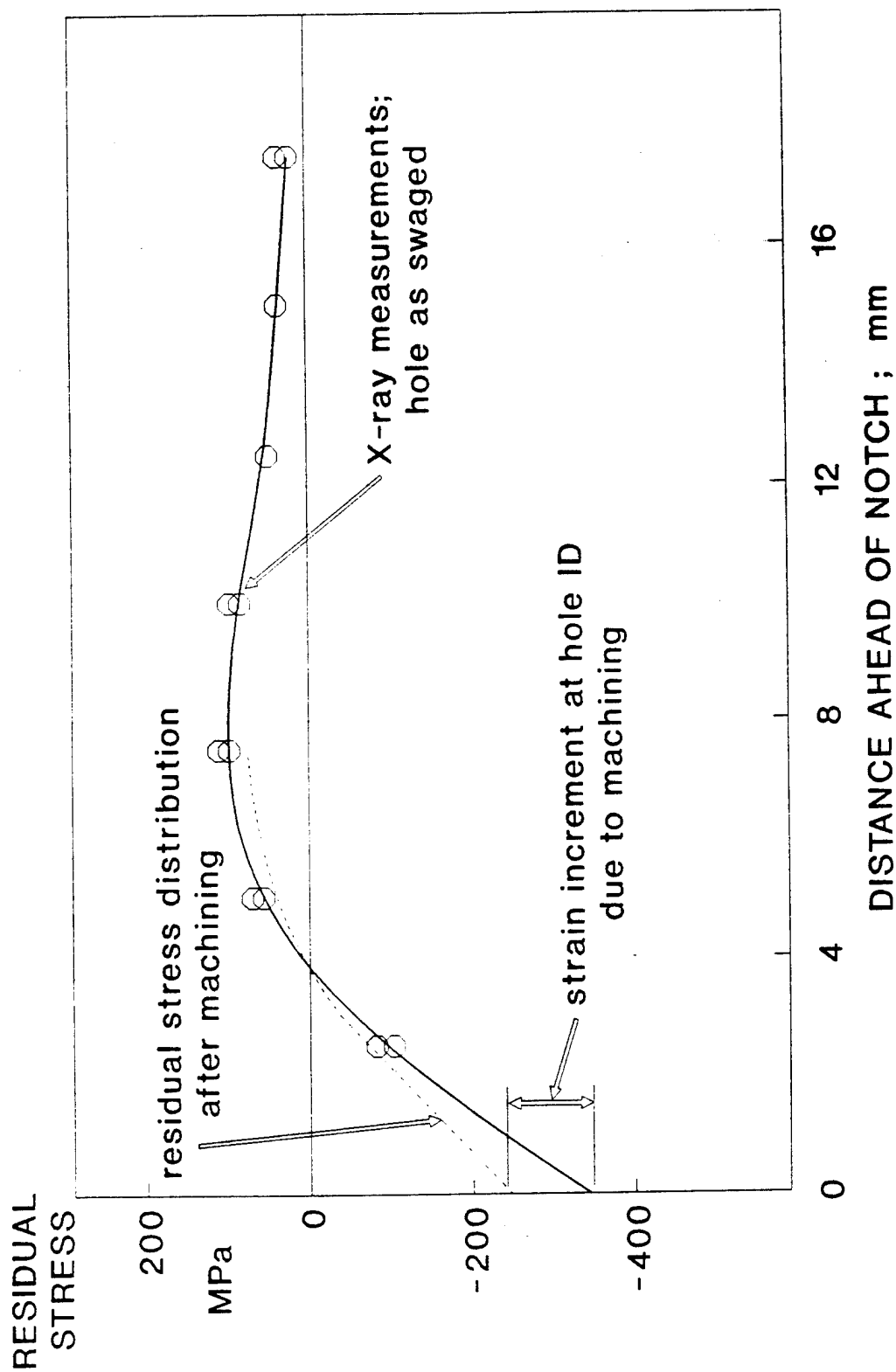


Figure 2. Measured residual stress for swaged and machined specimen.

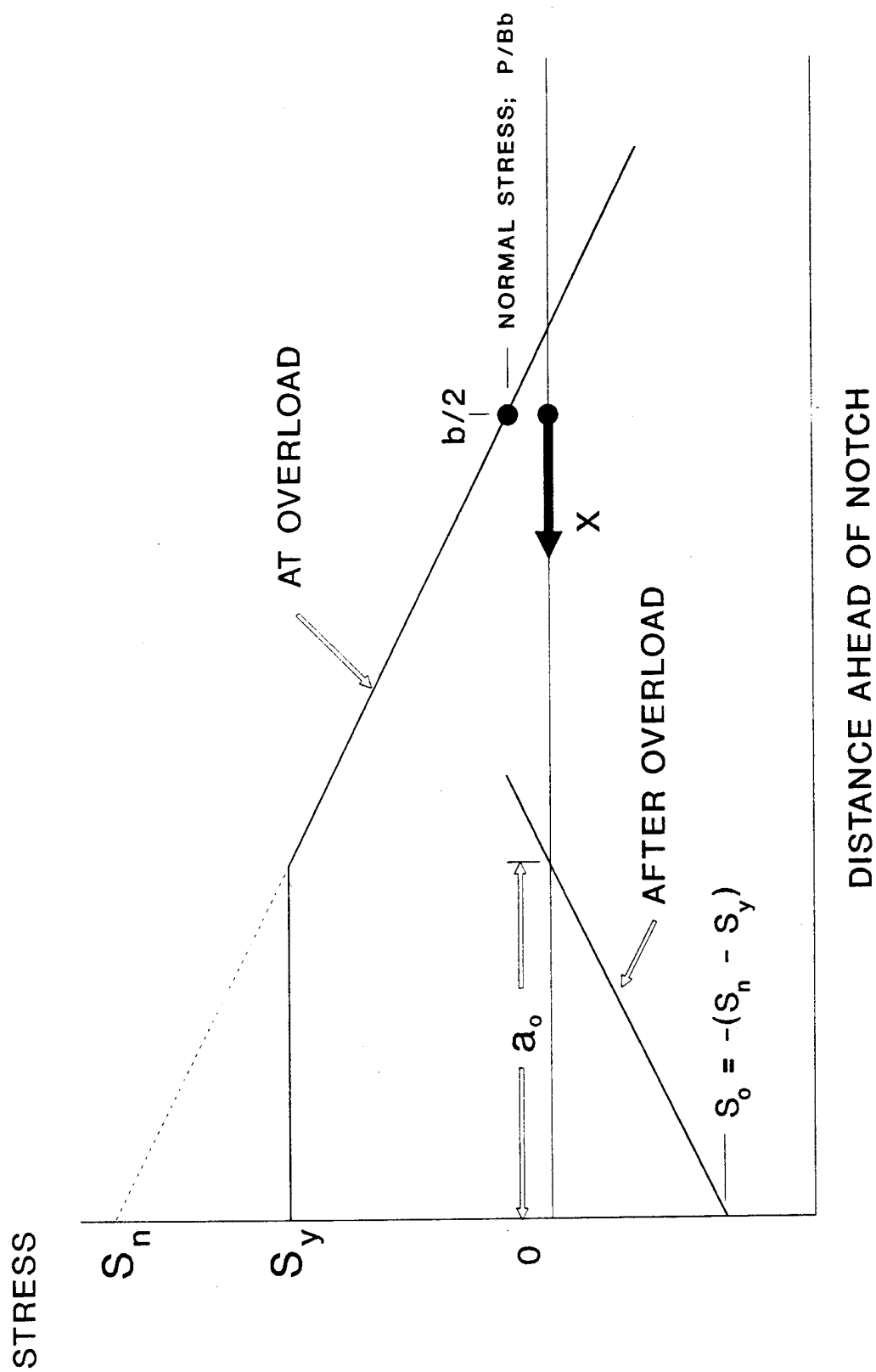


Figure 3. Model of elastic-plastic stresses due to overload of notch.

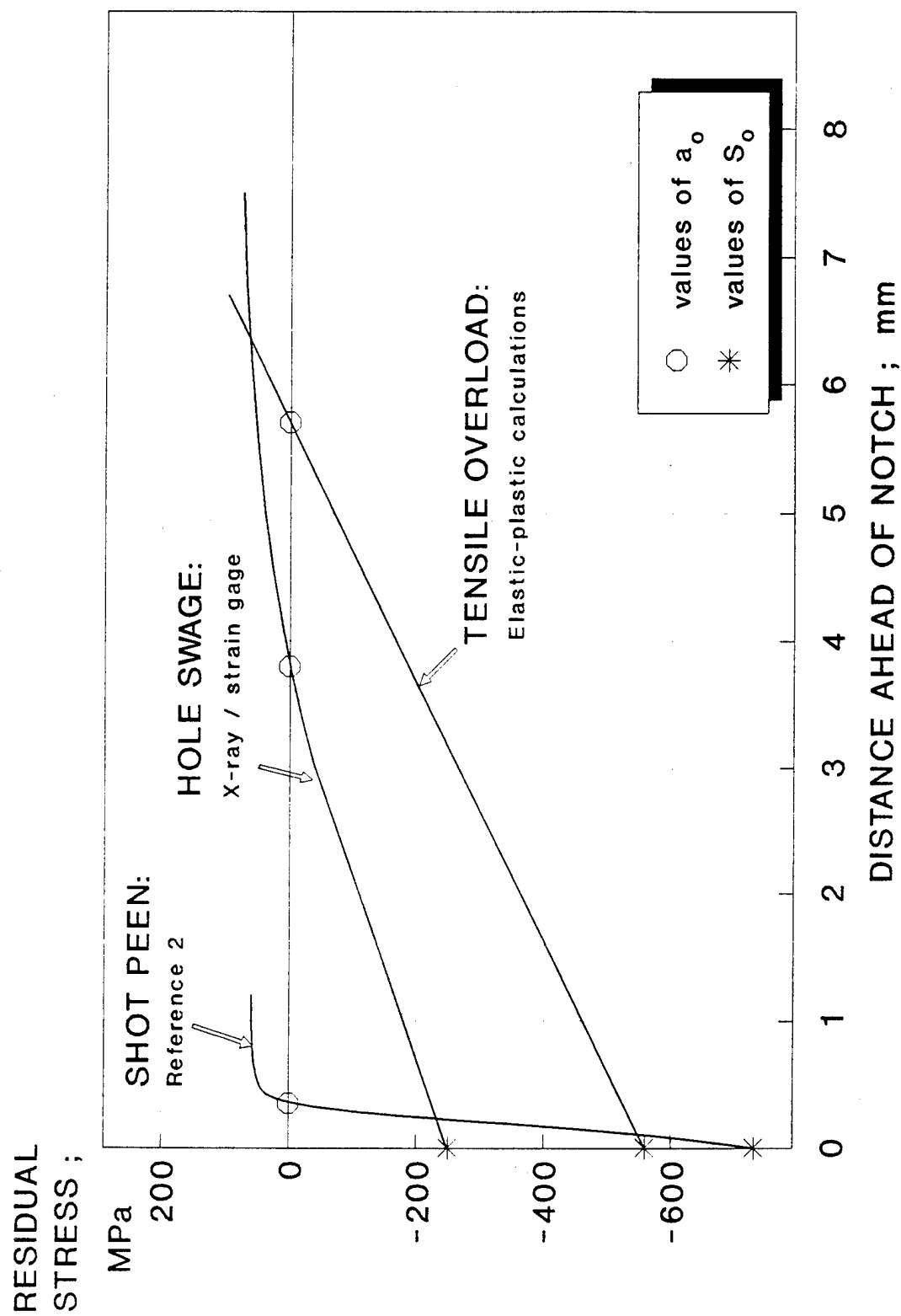


Figure 4. Typical residual stress distributions ahead of notch.

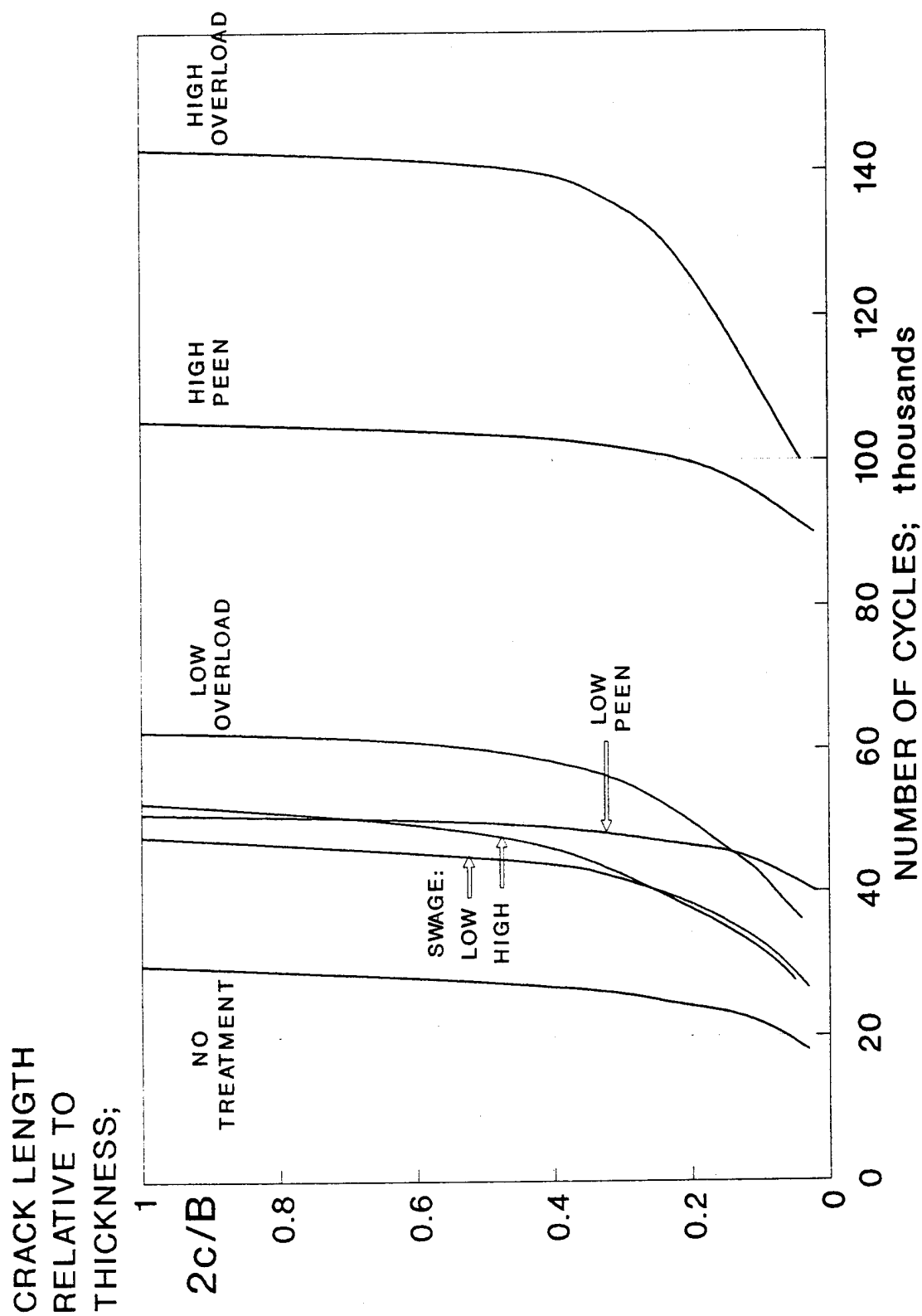


Figure 5. Measured fatigue crack growth for various notch root treatments.

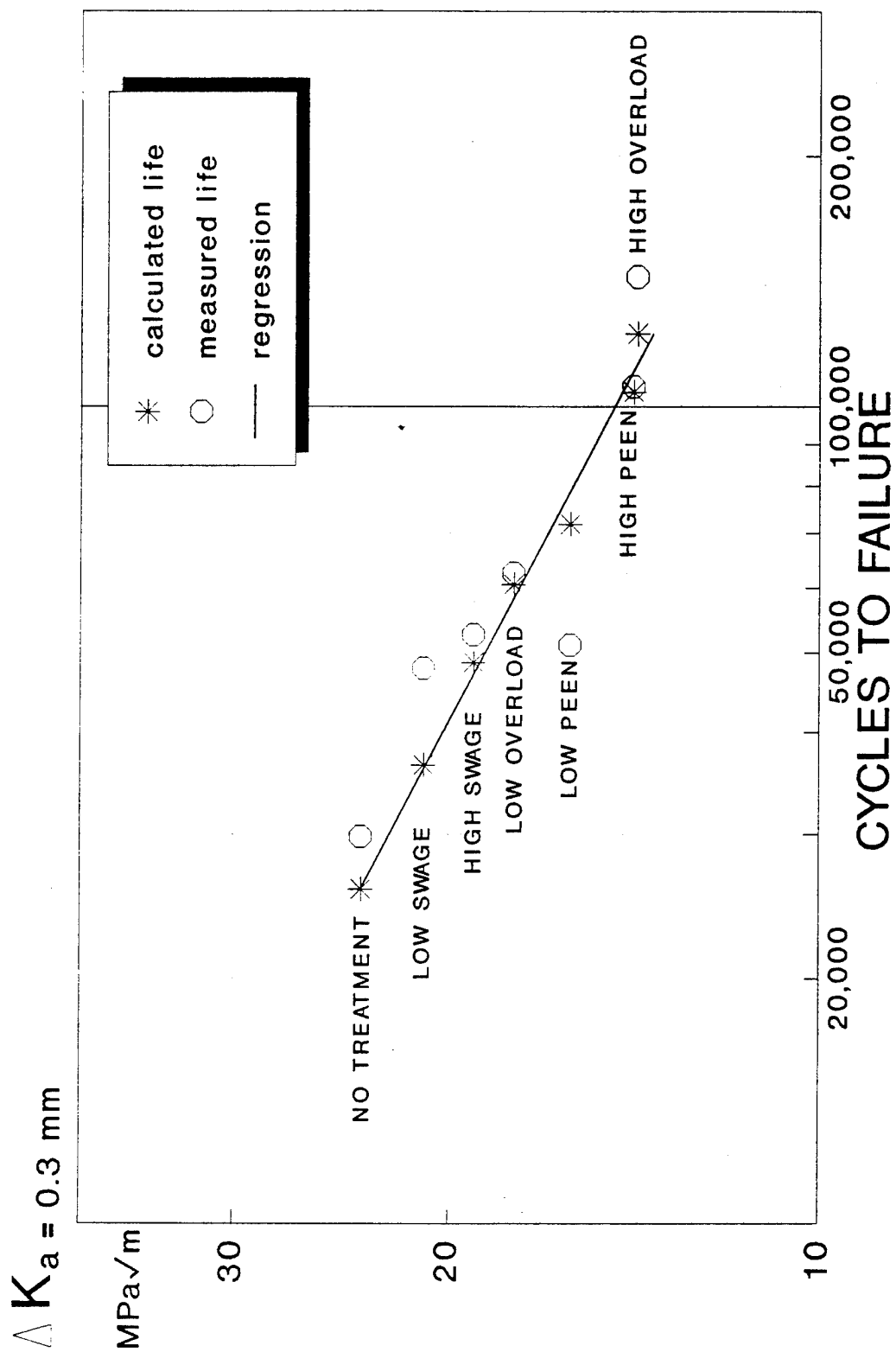


Figure 6. Comparison of measured and calculated fatigue lives.

TECHNICAL REPORT INTERNAL DISTRIBUTION LIST

	<u>NO. OF COPIES</u>
CHIEF, DEVELOPMENT ENGINEERING DIVISION	
ATTN: AMSTA-AR-CCB-DA	1
-DB	1
-DC	1
-DD	1
-DE	1
CHIEF, ENGINEERING DIVISION	
ATTN: AMSTA-AR-CCB-E	1
-EA	1
-EB	1
-EC	
CHIEF, TECHNOLOGY DIVISION	
ATTN: AMSTA-AR-CCB-T	2
-TA	1
-TB	1
-TC	1
TECHNICAL LIBRARY	
ATTN: AMSTA-AR-CCB-O	5
TECHNICAL PUBLICATIONS & EDITING SECTION	
ATTN: AMSTA-AR-CCB-O	3
OPERATIONS DIRECTORATE	
ATTN: SMCWV-ODP-P	1
DIRECTOR, PROCUREMENT & CONTRACTING DIRECTORATE	
ATTN: SMCWV-PP	1
DIRECTOR, PRODUCT ASSURANCE & TEST DIRECTORATE	
ATTN: SMCWV-QA	1

NOTE: PLEASE NOTIFY DIRECTOR, BENÉT LABORATORIES, ATTN: AMSTA-AR-CCB-O OF ADDRESS CHANGES.

TECHNICAL REPORT EXTERNAL DISTRIBUTION LIST

	<u>NO. OF COPIES</u>		<u>NO. OF COPIES</u>
ASST SEC OF THE ARMY RESEARCH AND DEVELOPMENT ATTN: DEPT FOR SCI AND TECH THE PENTAGON WASHINGTON, D.C. 20310-0103	1	COMMANDER ROCK ISLAND ARSENAL ATTN: SMCRI-ENM ROCK ISLAND, IL 61299-5000	1
ADMINISTRATOR DEFENSE TECHNICAL INFO CENTER ATTN: DTIC-OCP (ACQUISITION GROUP) BLDG. 5, CAMERON STATION ALEXANDRIA, VA 22304-6145	2	MIAC/CINDAS PURDUE UNIVERSITY P.O. BOX 2634 WEST LAFAYETTE, IN 47906	1
COMMANDER U.S. ARMY ARDEC ATTN: SMCAR-AEE	1	COMMANDER U.S. ARMY TANK-AUTMV R&D COMMAND ATTN: AMSTA-DDL (TECH LIBRARY) WARREN, MI 48397-5000	1
SMCAR-AES, BLDG. 321	1	COMMANDER U.S. MILITARY ACADEMY ATTN: DEPARTMENT OF MECHANICS WEST POINT, NY 10966-1792	1
SMCAR-AET-O, BLDG. 351N	1		
SMCAR-FSA	1		
SMCAR-FSM-E	1		
SMCAR-FSS-D, BLDG. 94	1		
SMCAR-IMI-I, (STINFO) BLDG. 59	2	U.S. ARMY MISSILE COMMAND REDSTONE SCIENTIFIC INFO CENTER ATTN: DOCUMENTS SECTION, BLDG. 4484 REDSTONE ARSENAL, AL 35898-5241	2
PICATINNY ARSENAL, NJ 07806-5000			
DIRECTOR U.S. ARMY RESEARCH LABORATORY ATTN: AMSRL-DD-T, BLDG. 305 ABERDEEN PROVING GROUND, MD 21005-5066	1	COMMANDER U.S. ARMY FOREIGN SCI & TECH CENTER ATTN: DRXST-SD 220 7TH STREET, N.E. CHARLOTTESVILLE, VA 22901	1
DIRECTOR U.S. ARMY RESEARCH LABORATORY ATTN: AMSRL-WT-PD (DR. B. BURNS) ABERDEEN PROVING GROUND, MD 21005-5066	1	COMMANDER U.S. ARMY LABCOM MATERIALS TECHNOLOGY LABORATORY ATTN: SLCMT-IML (TECH LIBRARY) WATERTOWN, MA 02172-0001	2
DIRECTOR U.S. MATERIEL SYSTEMS ANALYSIS ACTV ATTN: AMXSY-MP ABERDEEN PROVING GROUND, MD 21005-5071	1	COMMANDER U.S. ARMY LABCOM, ISA ATTN: SLCIS-IM-TL 2800 POWER MILL ROAD ADELPHI, MD 20783-1145	1

NOTE: PLEASE NOTIFY COMMANDER, ARMAMENT RESEARCH, DEVELOPMENT, AND ENGINEERING CENTER,
BENÉT LABORATORIES, CCAC, U.S. ARMY TANK-AUTOMOTIVE AND ARMAMENTS COMMAND,
AMSTA-AR-CCB-O, WATERVLIET, NY 12189-4050 OF ADDRESS CHANGES.

TECHNICAL REPORT EXTERNAL DISTRIBUTION LIST (CONT'D)

	<u>NO. OF COPIES</u>		<u>NO. OF COPIES</u>
COMMANDER		WRIGHT LABORATORY	
U.S. ARMY RESEARCH OFFICE		ARMAMENT DIRECTORATE	
ATTN: CHIEF, IPO	1	ATTN: WL/MNM	1
P.O. BOX 12211		EGLIN AFB, FL 32542-6810	
RESEARCH TRIANGLE PARK, NC 27709-2211			
DIRECTOR		WRIGHT LABORATORY	
U.S. NAVAL RESEARCH LABORATORY		ARMAMENT DIRECTORATE	
ATTN: MATERIALS SCI & TECH DIV	1	ATTN: WL/MNMF	1
CODE 26-27 (DOC LIBRARY)	1	EGLIN AFB, FL 32542-6810	
WASHINGTON, D.C. 20375			

NOTE: PLEASE NOTIFY COMMANDER, ARMAMENT RESEARCH, DEVELOPMENT, AND ENGINEERING CENTER,
BENÉT LABORATORIES, CCAC, U.S. ARMY TANK-AUTOMOTIVE AND ARMAMENTS COMMAND,
AMSTA-AR-CCB-O, WATERVLIET, NY 12189-4050 OF ADDRESS CHANGES.
